Financial Econometrics

On the Euro-Dollar Exchange Rate

Filippo Nardoni 0001172086 LM(EC)^2

22 December 2025

1 Introduction

This project provides an extensive analysis of the Euro–Dollar exchange rate using both daily and weekly data. The daily series spans from 1999 to 2025 (1999–01–04 to 2025–11–07), while the weekly series covers the period from (1999–01–04 to 2025–11–03). This allows us to examine the dynamics of one of the most significant currency pairs in the international monetary system. The U.S. dollar is the dominant currency due to its ability to anchor and influence the largest share of global financial transactions and reserves. By contrast, the euro is a relatively "young" currency, the product of a voluntary monetary union among European countries. Concentrating on this exchange rate is thus especially relevant. By analysing its statistical characteristics, we can determine models that consistently represent its behaviour, allowing us to generate dependable forecasts, build risk measures such as Value-at-Risk (VaR), and assess exceedances.

This work is organized into four main sections. Section 1 introduces the topic and provides background on exchange rates and their economic interpretation. Section 2 presents an empirical analysis based on daily data, focusing on the statistical and econometric properties of exchange rate returns. Section 3 extends the analysis to weekly data, allowing for a comparison across sampling frequencies. Finally, Section 4 is devoted to a discussion of bootstrap-based inference for the ARCH(1) model using the likelihood ratio test.

What is the exchange rate and what does it represent?

Understanding the exchange rate is fundamental for analysing the economic conditions of the countries involved in a currency pair, as well as for understanding the internal transmission of external inflation. The exchange rate of a currency y in terms of a currency x represents the price of one unit of currency y expressed in units of currency x. In our case, it measures how many U.S. dollars are required to purchase one euro.

$$EX_{x,y} = \frac{p_x}{p_y}$$

Ceteris paribus, if p_x increases relative to p_y, the exchange rate $EX_{x,y}$ rises. This implies that currency y becomes more expensive in terms of currency x: one needs more units of x to buy one unit of y. Equivalently, currency x depreciates while currency y appreciates. While it is beyond the scope of this project to provide a detailed discussion of exchange rate theory, it is important to highlight that the nominal exchange rate alone is insufficient to fully explain the dynamics of international currencies. A comprehensive analysis would require accounting for differences in price levels across countries, as these determine the real purchasing power of each currency.

Data collection and Data Handling

The data used in this analysis were obtained from the FRED database, from which we downloaded both daily and weekly USD/EUR exchange rate series. The daily dataset covers the period from 1999–01–04 to 2025–11–07, yielding a total of $T_d = 7005$ observations (consistent with approximately 252 trading days per year). The weekly dataset spans the period from 1999–01–04 to 2025–11–03, for a total of $T_w = 1401$ observations.

The raw FRED daily series contained 270 missing values (approximately 3.9% of the sample), while the weekly series contained 169 missing values (around 12.5% of the observations). All missing values were imputed using a local–mean smoothing procedure based on a moving average with a window size of 5:

$$\tilde{x}_t = \frac{1}{4} \sum_{i=\mathcal{W}}^{2} x_{t+i}, \quad \text{where, } \mathcal{W} = \{-2, -1, 1, 2\}$$

applied only to the missing entries. Once the data were cleaned and imputed, we proceeded with the empirical analysis.

2 Daily Analysis

Stationarity Analysis of Levels and Daily Returns

In this section, we consider the entire analysis of our daily data on the Euro/Dollar Exchange rate. We start by examining the series and running tests to identify the most essential features of the time series, which we aim to capture with our models. We start assessing the following graph:

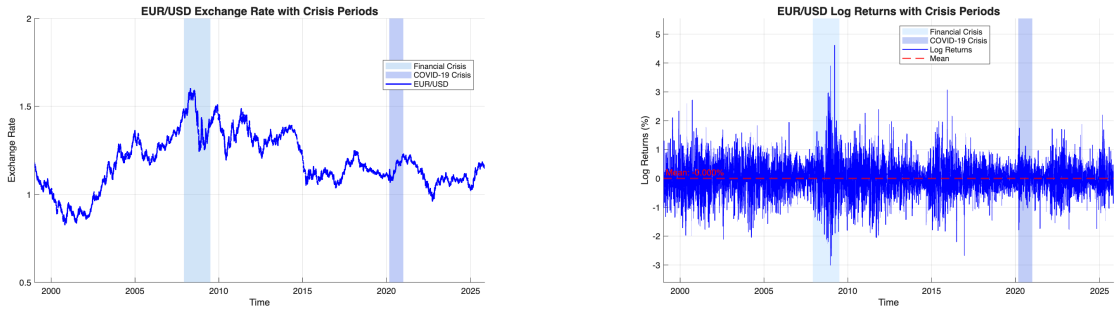

(a) EUR/DOL Exchange Rate (1999–2025)

(b) Exchange rate returns

Figure 1: Exchange rate series and corresponding returns.

Figure 1a illustrates that the exchange rate exhibits dynamics typical of a random walk, where its evolution is clearly governed by a stochastic trajectory rather than a stationary process. This indicates that the distribution of the series shifts in an unpredictable manner over time. Figure 1b, on the other hand, displays an apparent stability suggestive of stationarity, which would permit us to continue with our analysis. Nevertheless, relying solely on a visual judgment of stationarity is not a sufficiently robust approach; we therefore employ formal statistical tests to determine whether the time series is indeed stationary.

Table 1: Unit Root and Stationarity Tests on the Exchange Rate (Levels)

	DF	DF–Trend	ADF(5)	KPSS	VAR Ratio
p-value	0.550	0.676	0.567	0.010	0.832
Test Statistic	-0.277	-1.831	-0.232	114.39	0.212
Critical Value	-1.941	-3.413	-1.941	0.146	1.960
H_0	I(1)	I(1)	I(1)	I(0)	I(1)

In Table 1, several tests are presented that must be interpreted with caution, as they differ in both their testing procedures and in how they formulate the null hypothesis H_0 (see Appendix A for more details on each test). Focusing first on the initial column, which reports the standard Dickey-Fuller test with H_0: unit root, we are unable to reject the null hypothesis, thus indicating the presence of a unit root. Even when a trend is included, the test continues to fail to reject the unit root null at any conventional significance level $\alpha \in \{0.01, 0.05, 0.10\}$. By contrast, the KPSS test rejects its null hypothesis, since it is based on a different setup where the null is stationarity or integration of order zero, $I(0)$, thereby confirming that the series is non-stationary. Finally, the Variance Ratio Test does not reject the null hypothesis of a unit root.

Table 2: Unit Root and Stationarity Tests on the Exchange Rate (Returns)

	DF	DF–Trend	ADF(5)	KPSS	VAR Ratio
p-value	0.001	0.001	0.001	0.100	2.11×10^{-171}
Test Statistic	-83.369	-83.357	-34.217	0.0778	-27.908
Critical Value	-1.942	-3.413	-1.942	0.146	1.960

Table 2 reports the results of the same unit root and stationarity tests applied to the exchange rate returns, defined as[1]

$$\Delta ex_t = \frac{ex_t - ex_{t-1}}{ex_{t-1}}.$$

The results show that, in first differences, the Dickey–Fuller tests and the Variance Ratio test strongly reject the null of non-stationarity, with p-values well below 0.05 (and even 0.01). Conversely, we fail to reject the KPSS test, which maintains the null of stationarity. Taken together, all tests consistently indicate that the differenced exchange rate series is stationary.

Since the unit root tests indicate that the exchange rate is integrated of order one, $I(1)$, its first difference—interpreted as the *exchange rate return*—appears to be stationary. We therefore work with daily exchange rate returns for the remainder of the analysis.

An additional question concerns whether returns are uncorrelated, or even whether they can be treated as independent. To investigate this, we first examine the correlogram to assess whether autocorrelations at different lags are statistically significant. We then proceed to explore whether exchange rate returns may exhibit independence by applying a nonlinear transformation of the returns using a function $f(x)$, which we specify as $f(x) = x^2$.

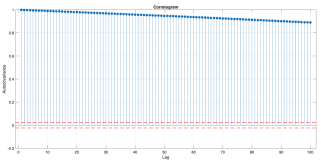

(a) Correlogram: Exchange rate in Levels

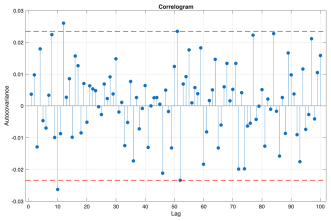

(b) Correlogram: First Differences

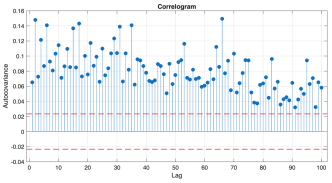

(c) Correlogram: First difference squared

Figure 2: Correlograms for the Daily Exchange Rate Series

Figure 2c reports the correlogram of the exchange rate in levels up to lag 100. The autocorrelations display a long and slowly decaying (and persistent) pattern, which is a typical feature of non-stationary time series. In contrast, Figure 2b shows the correlogram of the first differences. Here, although a few autocorrelations at short lags are statistically significant, the overall pattern indicates that the $I(1)$ process has virtually no memory, implying no linear relationship between ex_t and ex_{t-k}.

However, the absence of linear autocorrelation does not imply[2] independence. Stochastic independence between two variables X and Y requires that

$$\text{Cov}\left(f(X),\, g(Y)\right) = 0 \quad \forall\, f(\cdot), g(\cdot),$$

i.e. all nonlinear transformations must also be uncorrelated. To investigate this, we analyse the autocorrelation of squared returns. Figure 2a shows that ex_t^2 exhibits strong and slowly decaying autocorrelations, revealing nonlinear dependence in the form of volatility clustering, even though the raw returns themselves appear uncorrelated.

[1] We do not use log-differences for two reasons: (1) variations in the exchange rate frequently exceed 10%, for which the logarithmic approximation would be inaccurate; (2) using simple differences allows us to exploit the identity $\Delta ex_{t,t-k} = \sum_{i=1}^{k} \Delta ex_{t-i}$.

[2] We recall that Independence $\implies$ Uncorrelation

Distribution of daily exchange rate returns

In this section, we analyse the distribution of exchange rate returns. In particular, we proceed by examining the empirical moments of the data to detect some features related to symmetry/asymmetry and the presence of extreme values in the tails.

Mean	Std. Dev.	Skewness	Kurtosis
-0.00028568	0.31648	0.14805	5.6313

Table 3: Summary Statistics

From Table 3, we observe that the sample mean is essentially zero, which is expected for a return series. The second moment reports a standard deviation of approximately 0.316, capturing the volatility of the daily returns. The skewness is positive ($s = 0.148$), indicating a slight asymmetry in the distribution: returns display a longer right tail, meaning that large positive realizations are somewhat more frequent than large negative ones. Finally, the kurtosis ($k = 5.63$) substantially exceeds the Gaussian reference value of 3, indicating pronounced heavy tails. This aligns with a well-established stylised fact in financial time series: returns generally exhibit leptokurtic behaviour. Additional insight comes from the following figure:

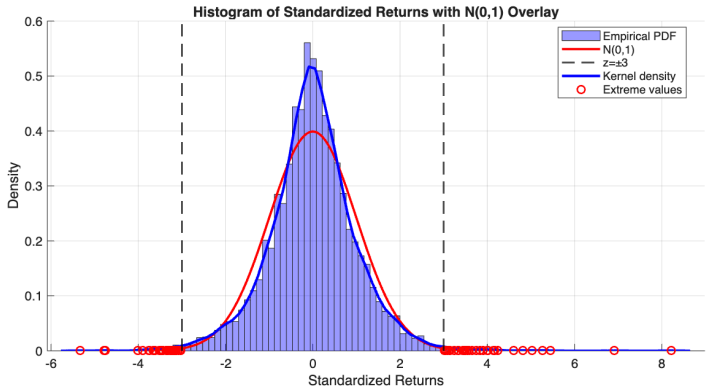

Figure 3: Histogram of Standardised Returns with Gaussian and Kernel Density Estimates

Figure 6 reports the distribution of the standardised returns, $z_t = \frac{ex_t - \bar{x}}{\hat{\sigma}_z}$, which are centered around zero and scaled to unit variance. We overlay the $N(0,1)$ density and the empirical kernel density estimator, computed with a Gaussian kernel and an optimal bandwidth of $h = 0.1455$. The kernel estimator is defined as

$$\widehat{F}_h(x) = \frac{1}{n}\sum_{i=1}^{n} G\left(\frac{x - x_i}{h}\right), \qquad G(x) = \int_{-\infty}^{x} K(t)\, dt.$$

The empirical density exhibits a higher concentration around the center and noticeably heavier tails relative to the Gaussian benchmark, suggesting significant deviations from normality. To further quantify tail behaviour, we compute the number of observations falling beyond ± 3 standard deviations, which in the figure are shown as red points:

$$c^- = \sum_{i=1}^{n} \mathbf{1}\{z_i < -3\}, \qquad c^+ = \sum_{i=1}^{n} \mathbf{1}\{z_i > 3\}.$$

We obtain $c^- = 36$ and $c^+ = 38$, for a total of $c_{\text{tot}} = 74$ extreme observations. Relative to the sample size, the proportion is

$$\frac{c_{\text{tot}}}{n} = \frac{74}{7005} \approx 0.0106 \quad (\text{or } 1.06\%).$$

Under normality, however, we would expect only about 0.27% of observations outside the ± 3 standard deviation range. The fact that we observe more than four times this amount provides strong evidence of fat-tailed behaviour, in line with the excess kurtosis previously discussed. As suggested from our

previous analysis, we study the behaviour of our distribution in the tails [Loretan and Phillips, 1994], so we assume Pareto-type Tails, imposing therefore:

$$P(X > x) \propto cx^{-\alpha}$$

where α controls the decay rate of the tails. We can prove that the Tail index expresses important information regarding the existence of the moments; therefore, to estimate it, we use the Hill estimator, which is obtained by running the following regression:

$$\log\left(\frac{m}{T}\right) = C - \alpha \log(x_{(m)})$$

We estimate the tail index using the Hill estimator based on the ordered statistics of the left tail, denoted by $x_{(1)} \leq x_{(2)} \leq \cdots \leq x_{(m)}$. From our analysis, we obtain $\hat{\alpha} = 6.5499$, which implies that the distribution has finite moments only up to order $p < \hat{\alpha}$. Hence, moments up to the sixth order exist, while higher-order moments (such as the seventh moment) become infinite under the assumption of regularly varying tails.

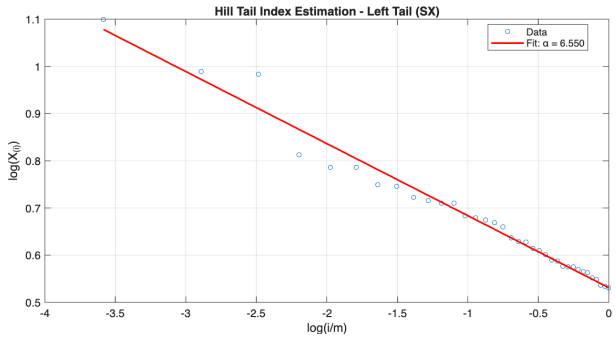

Figure 4: Fitted regression line of the Hill estimator on the log transformation of the data

Figure 6 displays the Hill plot for the left tail. The scatter points correspond to the log–log transformation of the m extreme order statistics, while the fitted line corresponds to the Pareto tail approximation. The slope of this regression yields the Hill estimate $\hat{\alpha} = 6.55$. The approximately linear relationship supports the presence of regularly varying tails, and the estimated tail index indicates moderately heavy tails, consistent with the earlier excess kurtosis.

Table 4 reports the results of three widely used normality tests.

Test	**Statistic**	**p-value**	**Reject** H_0
Jarque–Bera	2048.7	0.001	1
Kolmogorov–Smirnov	0.04728	4.7102×10^{-14}	1
Cramér–von Mises	5.8927	3.5788×10^{-16}	1

Table 4: Normality Test Results

We further investigate the distributional properties of our exchange rate returns using various normality tests. We start with the Jarque-Bera test, which is based on the third and fourth moments of the distribution and therefore detects departures from normality due to excessive skewness or kurtosis. The Kolmogorov–Smirnov test instead compares the empirical distribution function with the theoretical $N(0, 1)$ distribution, capturing global deviations in shape. Finally, the Cramér–von Mises statistic measures the integrated squared distance between the empirical and theoretical cumulative distribution functions, providing sensitivity to discrepancies across the entire support.

Across all tests, the null hypothesis of normality is strongly rejected, with extremely small p-values. This reinforces the earlier evidence from sample kurtosis, tail analysis, and kernel density estimation: the distribution of standardised returns clearly departs from normality, exhibiting heavy tails and non-Gaussian features typical of financial time series.

Financial Modeling

In the previous section, we have studied several features of the returns, focusing in particular on whether the series can be regarded as approximately normal. We now turn to econometric models that allow us to capture the main characteristics of the exchange rate returns series.

We begin by restricting attention to the first two-thirds of the sample, i.e. we consider observations $t = 1, \dots, t_f$, where $t_f = 2 \cdot \lfloor T/3 \rfloor$. On this subsample, we adopt a data-driven approach to select the conditional volatility model that best fits our setting. Specifically, we consider the following GARCH specification:

$$\begin{cases} x_t = \sigma_t z_t, \quad \text{with } z_t \sim i.i.d. \text{ such that } E[z_t] = 0,\ V[z_t] = 1, \\ \sigma_t^2 = \omega_0 + \sum_{i=1}^{p} \alpha_i x_{t-i}^2 + \sum_{j=1}^{q} \beta_j \sigma_{t-j}^2, \end{cases} \tag{1}$$

where the lag orders (p, q) of the GARCH(p, q) model [Bollerslev, 1986] are left unspecified and will be chosen using information criteria.

To this end, we estimate (1) over a fine grid of lags $p, q \in \{1, \dots, 10\}$ and compute the AIC and BIC for each specification. The resulting selection surfaces are reported in Figure 5.

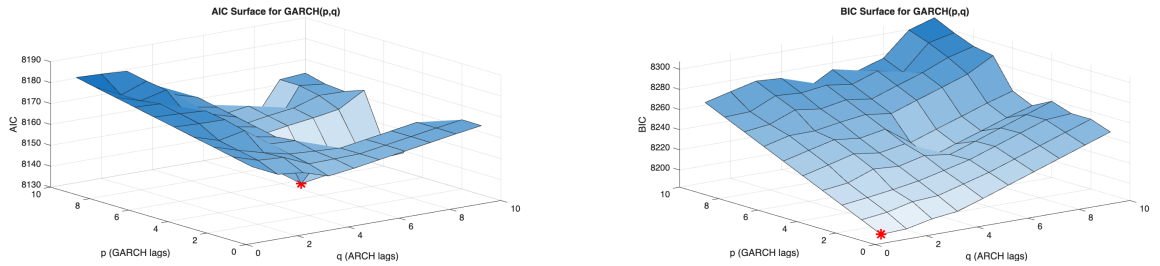

(a) AIC surface for GARCH(p, q) (b) BIC surface for GARCH(p, q)

Figure 5: Model selection surfaces for GARCH(p, q)

Over the grid $p, q \in [1, 10]$, the AIC selects a relatively rich GARCH$(5, 6)$ specification, whereas the BIC favours the more parsimonious GARCH$(1, 1)$ model as the one that best fits the data. Given the well-known tendency of AIC to overfit and the widespread use of GARCH$(1, 1)$ in the literature, our baseline choice is to adopt the GARCH$(1, 1)$ specification. We then extend this baseline model to allow for possible asymmetries in the volatility response to positive and negative shocks by considering the GJR-GARCH model, introduced by [Glosten et al., 1993]. The GJR-GARCH$(1, 1)$ differs from (1) only in the specification of the conditional variance, which is given by

$$\sigma_t^2 = \omega_0 + \alpha_1 x_{t-1}^2 + \rho\, x_{t-1}^2 \mathbf{1}\{x_{t-1} < 0\} + \beta_1 \sigma_{t-1}^2, \tag{2}$$

where $\mathbf{1}\{x_{t-1} < 0\}$ is an indicator function that equals 1 when the lagged return is negative and 0 otherwise. The coefficient ρ captures asymmetry in the volatility response (the leverage effect). Note that GARCH$(1, 1)$ is nested within GJR-GARCH$(1, 1)$ as the special case $\rho = 0$, so that a likelihood ratio test can be used to compare the two models and assess whether including the asymmetry term improves the fit.

As shown in Table 5, both the GARCH(1,1) and the GJR–GARCH(1,1) specifications exhibit a relatively small ARCH coefficient and a much larger GARCH coefficient. In the symmetric GARCH(1,1) model, the estimate of the ARCH parameter is $\hat{\alpha}_1 = 0.02834$ (s.e. $= 0.00289$), while the persistence parameter is $\hat{\beta}_1 = 0.96892$ (s.e. $= 0.00279$). A similar pattern emerges in the asymmetric specification, where $\hat{\alpha}_1 = 0.01971$ (s.e. $= 0.00283$) and $\hat{\beta}_1 = 0.97089$ (s.e. $= 0.00416$).

This configuration is fully consistent with the stylized facts of financial return series: volatility persistence is primarily driven by the GARCH component β_1, which captures the slow-moving dynamics of the conditional variance, while the impact of recent shocks x_{t-1}^2—as measured by α_1—is comparatively limited once persistence in σ_t^2 is accounted for.

For both models, the sum of the ARCH and GARCH coefficients is close to, but strictly below, unity:

$$\phi^{\text{GARCH}} = \hat{\alpha}_1 + \hat{\beta}_1 = 0.02834 + 0.96892 = 0.99724 < 1, \qquad \phi^{\text{GJR}} = \hat{\alpha}_1 + \hat{\beta}_1 = 0.01971 + 0.97089 = 0.99060 < 1.$$

Table 5: Estimated GARCH-Type Volatility Models

	GARCH(1,1)		**GJR–GARCH(1,1)**	
Parameter	Estimate	t-stat	Estimate	t-stat
ω	0.00110 (0.00021)	5.238 [0.000]	0.00097 (0.00021)	4.582 [0.000]
α	0.02834 (0.00289)	9.823 [0.000]	0.01971 (0.00283)	6.975 [0.000]
ρ (leverage)	— —	— —	0.01404 (0.00315)	4.454 [0.00001]
β	0.96892 (0.00279)	347.64 [0.000]	0.97089 (0.00416)	233.16 [0.000]
Log-likelihood	–4078.20		–4074.20	

Notes: The table reports quasi-maximum likelihood estimates of a standard GARCH(1,1) model and a GJR–GARCH(1,1) model. Standard errors are reported in parentheses, and p-values are reported in square brackets. The parameter ρ captures asymmetric (leverage) effects in conditional volatility. All models are estimated under conditional Gaussianity.

These values ensure weak stationarity (as well as strict stationarity since $E[\log(\alpha z^2 + \beta)] < 0$) of the conditional variance process in both cases, while at the same time indicating a high degree of volatility persistence, especially for the symmetric GARCH model.

An important additional feature emerges from the GJR–GARCH(1,1) specification. The asymmetry parameter is estimated as $\hat{\rho} = 0.01404$ with a standard error of 0.00315, yielding a t-statistic of 4.45 and a p-value below 0.01. This provides strong statistical evidence of asymmetric volatility responses: negative shocks have a larger effect on future volatility than positive shocks of the same magnitude, in line with the well-documented leverage effect in financial markets.

From a model comparison perspective, the log-likelihood improves from -4078.20 under the GARCH(1,1) specification to -4074.20 under the GJR–GARCH(1,1). The resulting likelihood ratio statistic equals 8.04, which exceeds the 5% critical value of 3.84 for a $\chi^2(1)$ distribution. Hence, the null hypothesis of symmetry is rejected, indicating that allowing for asymmetric effects leads to a statistically significant improvement in model fit.

Taken together, the statistical significance of the asymmetry parameter and the likelihood-ratio test results support the GJR-GARCH (1,1) as the preferred specification for modelling the conditional volatility of returns in this application. Before proceeding with further applications of our model, we analyse the standardized returns $\hat{z}_t = \frac{x_t}{\hat{\sigma}_t}$, obtaining the results from the table below:

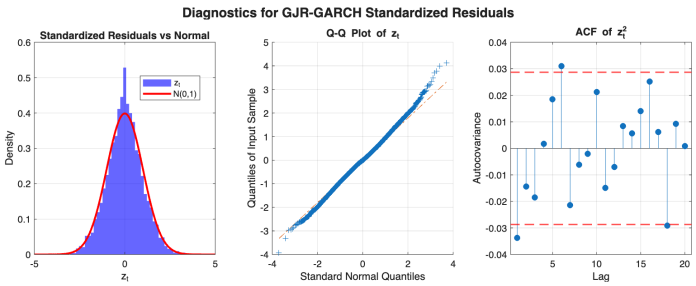

Figure 6: GJR-GARCH standardised returns diagnostic

Here we note that the normality assumption for z_t may be inappropriate; The histogram and the Q–Q plot indicate noticeable deviations from Gaussianity, particularly in the tails, suggesting the presence of excess kurtosis. This evidence implies that the conditional normality assumption for z_t may be restrictive, and that a Student–t distribution or another heavy–tailed specification could provide a more adequate description of the conditional distribution.

The autocorrelation function of the squared standardized residuals $\hat{z}_t^2$ exhibits a small number of marginally significant correlations at low lags. This pattern points to the possible presence of residual

conditional heteroskedasticity, indicating that the variance equation may not fully capture the dynamics of volatility.

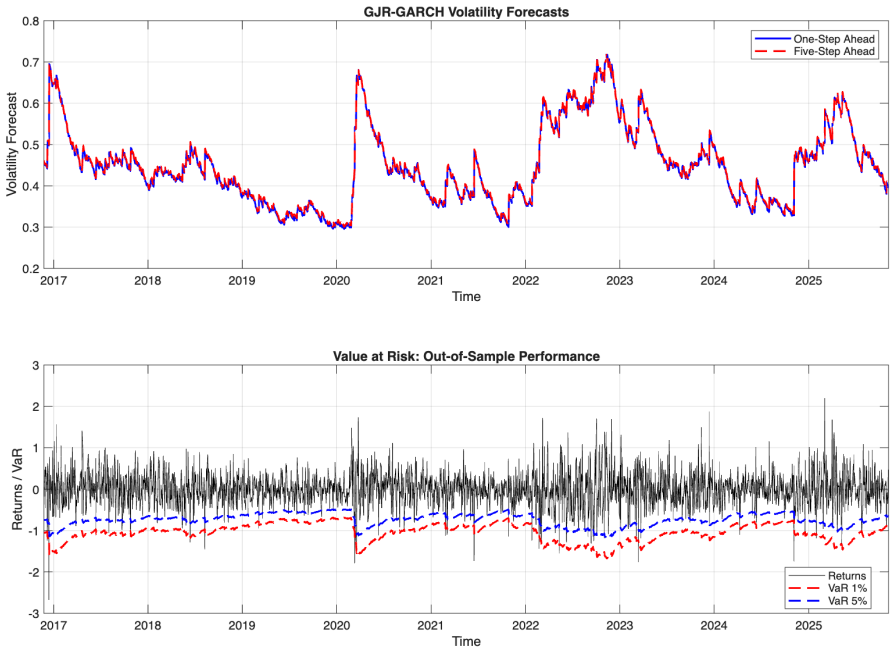

Figure 7: Forecast using GJR-GARCH and VaR at 1% and 5%

Figure 7 reports the out-of-sample volatility and risk forecasts obtained from the estimated GJR–GARCH(1,1) model. The one-step-ahead and five-step-ahead conditional volatility forecasts display a high degree of persistence and closely track periods of market stress, reflecting the large estimated value of the persistence parameter $\hat{\alpha}_1 + \hat{\beta}_1 + \frac{1}{2}\hat{\rho}$. In terms of forecast accuracy, the mean squared forecast error (MSFE) of the one-step-ahead conditional variance forecasts equals 0.1448, indicating a satisfactory predictive performance for daily volatility.

The lower panel of Figure 7 reports the one-step-ahead Value at Risk (VaR) forecasts at the 1% and 5% confidence levels, computed under the conditional Gaussian assumption as

$$\mathrm{VaR}_{t+1|t}(\alpha) = -\hat{\sigma}_{t+1|t}\,\Phi^{-1}(\alpha), \qquad \alpha \in \{0.01,\, 0.05\}.$$

The validity of the VaR forecasts is assessed by comparing the realized returns with the predicted VaR thresholds. At the 1% level, 25 exceedances are observed, corresponding to an empirical exceedance rate of 1.07%, which is very close to the nominal level of 1%. This indicates an excellent calibration of extreme downside risk.

At the 5% level, 89 exceedances are recorded, yielding an empirical exceedance rate of 3.81%, which is below the nominal rate of 5%. This suggests a mildly conservative behavior of the model at intermediate quantiles, with the VaR thresholds tending to slightly overestimate risk. Overall, the exceedance frequencies remain reasonably close to their theoretical counterparts, supporting the adequacy of the GJR–GARCH(1,1) model for risk forecasting purposes.

Taken together, the volatility forecasting performance and the VaR exceedance results confirm that accounting for asymmetric volatility dynamics improves the accuracy and reliability of both conditional variance and downside risk forecasts in the out-of-sample period.

3 Weekly Analysis

Stationarity Analysis

In this section, we provide an intensive analysis of weekly data from the same exchange rate. Employing weekly data for the same window of time we reduce the observation to $T = 1401$.

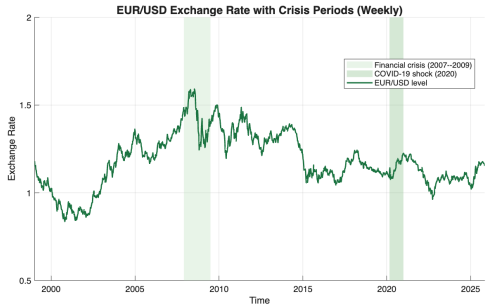

(a) EUR/DOL Exchange Rate (1999–2025)

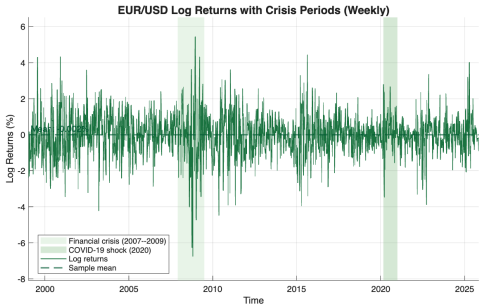

(b) Exchange rate returns

Figure 8: Exchange rate (weekly) series and corresponding returns.

From Figure 8, it can be seen that the main stylised facts observed in the daily data are largely preserved at the weekly frequency. In particular, the exchange rate exhibits pronounced persistence in levels and volatility clustering in returns.

An overview of the stationarity properties of the series is provided in Tables 6 and Figure 9. The results clearly indicate that the exchange rate is non-stationary in levels. Standard Dickey–Fuller and augmented Dickey–Fuller tests fail to reject the null hypothesis of a unit root, both with and without a deterministic trend, while the variance ratio test also does not reject the random walk hypothesis. Taken together, these findings are consistent with the view that the exchange rate is an integrated process.

By contrast, the exchange rate returns display strong evidence of stationarity. The unit root null is decisively rejected by the Dickey–Fuller and augmented Dickey–Fuller tests, while the KPSS test does not provide evidence against stationarity. Moreover, the variance ratio test strongly rejects the random walk hypothesis. Overall, these results support the conclusion that the exchange rate is integrated of order one ($I(1)$) with stationary returns.

Table 6: Unit Root and Random Walk Tests on Exchange Rate Levels (Weekly)

	DF	DF–Trend	KPSS	ADF(5)	Variance Ratio
p-value	0.56693	0.68053	0.01000	0.57507	0.60656
Test statistic	−0.23215	−1.82210	22.93500	−0.20994	−0.51499
Critical value (5%)	−1.94160	−3.41440	0.14600	−1.94160	1.96000

After discussing stationarity, we proceed to analyse the series's correlogram and the implied transformed versions using returns and the square of returns.

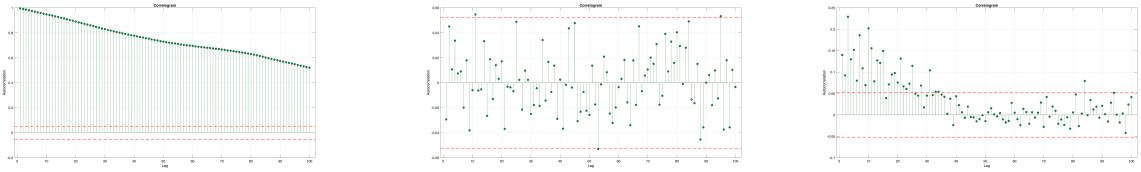

(a) Exchange rate levels (b) Returns (c) Square returns

Figure 9: Correlograms of the weekly EUR/USD exchange rate: levels, returns, and square returns.

As with the daily data, the correlogram of the exchange rate in levels shows strong, slowly decaying autocorrelations, indicating a high degree of persistence. This behaviour is typical of unit root processes,

in which shocks have permanent effects, and is fully consistent with the non-stationarity results obtained in the previous analysis.

In contrast, the correlogram of exchange rate returns shows very weak serial correlation at all lags, with only a small number of autocorrelations marginally exceeding the statistical significance bounds. This pattern supports the view that returns are approximately serially uncorrelated.

Finally, the correlogram of squared returns reveals substantial and persistent dependence, indicating strong serial correlation in second moments. This provides clear evidence of volatility clustering and motivates the use of conditional heteroskedasticity models, such as ARCH and GARCH, for modelling the dynamics of the exchange rate volatility.

Distribution of Weekly returns

We now proceed with the analysis of the unconditional distribution of weekly exchange rate returns.

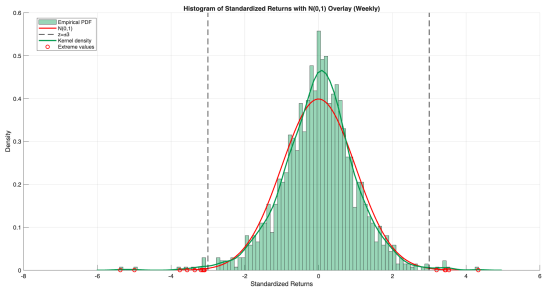

Figure 10: Histogram of weekly exchange rate returns with Gaussian benchmark

Figure 10 shows the empirical distribution of weekly returns. The distribution exhibits a pronounced concentration of observations around the mean and markedly heavier tails than those implied by the Gaussian distribution. Also, we can observe circled in red observations with scores higher than 3 standard deviations. Such features are well documented in financial return series and suggest departures from normality driven by excess kurtosis and asymmetry.

To further characterise the distributional properties of returns, Table 7 reports the estimated first four moments. The mean return is close to zero, while the standard deviation indicates substantial weekly variability. The negative skewness indicates a slight asymmetry toward negative returns, whereas the kurtosis substantially exceeds the Gaussian benchmark of three, confirming the presence of fat tails.

Table 7: First Four Moments of Weekly Exchange Rate Returns

Mean (μ)	Std. Dev. (σ)	Skewness	Kurtosis
-0.0017	1.5718	-0.2416	4.8012

Formal evidence against normality is provided by a battery of distributional tests reported in Table 8. The Jarque–Bera, Kolmogorov–Smirnov, and Cramér–von Mises tests all strongly reject the null hypothesis of Gaussianity at conventional significance levels. These results reinforce the visual evidence from the histogram and the moment-based analysis, highlighting the inadequacy of the normal distribution for modelling exchange rate returns.

Table 8: Normality Tests on Weekly Exchange Rate Returns

Test	Statistic	p-value	Reject H_0
Jarque–Bera	204.35	0.001	Yes
Kolmogorov–Smirnov	0.0379	0.0350	Yes
Cramér–von Mises	0.6857	0.0133	Yes

Financial Modeling

Once the main characteristics of the series have been documented, we proceed to specify financial econometric models capable of capturing the observed volatility dynamics. As in the analysis based on daily data, we consider parametric conditional heteroskedasticity models that are well-suited to capturing volatility clustering and return persistence.

Model selection is carried out using standard information criteria. Referring to Equation (1), we estimate a range of GARCH(p, q) specifications and evaluate their relative performance using the Akaike Information Criterion (AIC) and the Bayesian Information Criterion (BIC). The resulting information-criterion surfaces are reported in Figure 11.

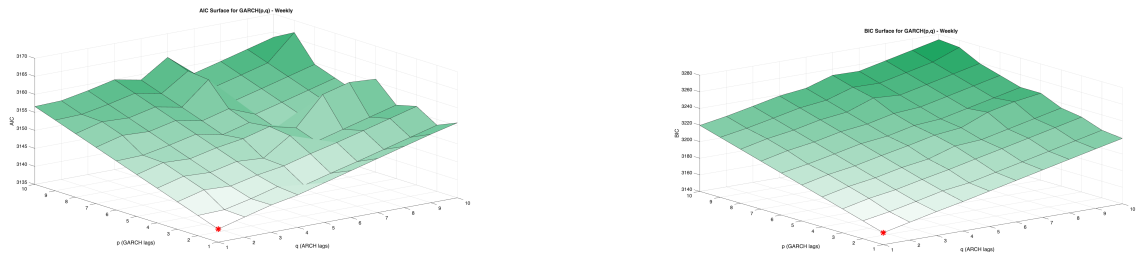

(a) AIC surface

(b) BIC surface

Figure 11: Information-criterion surfaces for GARCH(p, q) models estimated on weekly exchange rate returns.

Both criteria select a parsimonious specification. In particular, the minimum of both the AIC and the BIC surfaces is attained at $(p, q) = (1, 1)$, indicating that a GARCH(1,1) model provides an adequate balance between goodness of fit and model complexity for weekly exchange rate returns.

Table 9: Estimated GARCH-Type Volatility Models (Weekly)

	GARCH(1,1)		**GJR–GARCH(1,1)**	
Parameter	Estimate	t-stat	Estimate	t-stat
ω	0.0356	1.8092	0.0340	1.8089
	(0.0197)	[0.0704]	(0.0188)	[0.0705]
α	0.0856	3.8548	0.0678	3.1441
	(0.0222)	[0.0001]	(0.0216)	[0.0017]
γ (leverage)	—	—	0.0233	1.1322
	—	—	(0.0206)	[0.2576]
β	0.8975	51.3830	0.9035	46.3940
	(0.0175)	[0.0000]	(0.0195)	[0.0000]
Log-likelihood	−1566.30		−1565.80	

Notes: The table reports quasi-maximum likelihood estimates of a GARCH(1,1) model and a GJR–GARCH(1,1) model estimated on weekly exchange rate returns. Standard errors are reported in parentheses, and p-values are reported in square brackets. The parameter γ captures asymmetric (leverage) effects in conditional volatility. Estimation is conducted under conditional Gaussianity.

The estimation results for the GARCH(1,1) and GJR–GARCH(1,1) models are reported in Table 9. In both specifications, the estimated GARCH coefficient α is positive and statistically significant, indicating that past shocks to returns contribute to current volatility. The GARCH coefficient β is large and highly significant in both models, indicating strong volatility persistence. As a result, the conditional variance exhibits slow mean reversion, a feature commonly observed in financial return series.

In the asymmetric GJR–GARCH model, the leverage parameter γ is positive but not statistically significant at conventional levels. This suggests that, at the weekly frequency, negative shocks do not generate a substantially different volatility response compared to positive shocks of the same magnitude.

Hence, while the asymmetric specification allows for richer dynamics, the data provide only weak evidence in favour of asymmetric volatility effects.

Model comparison based on the log-likelihood values shows a slight improvement when moving from the symmetric GARCH model ($\ell = -1566.3$) to the GJR–GARCH model ($\ell = -1565.8$). The corresponding likelihood ratio statistic equals $LR = 0.975$, which is well below the 5% critical value of 3.84 from a $\chi^2(1)$ distribution. Therefore, the null hypothesis of symmetry cannot be rejected, indicating that the additional asymmetry parameter in the GJR-GARCH model does not yield a statistically significant improvement in fit.

Overall, both models capture the main features of weekly exchange rate volatility. However, given the lack of statistical evidence supporting asymmetric effects and the principle of parsimony, the symmetric GARCH(1,1) model is preferred for subsequent analysis.

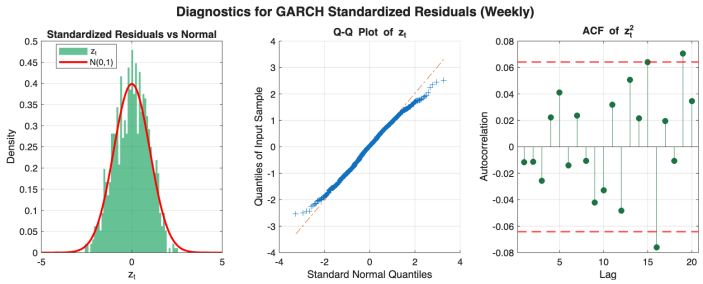

Figure 12: GARCH(1,1) diagnostic on standardized residuals

Figure 12 presents a graphical diagnostic of the standardized residuals. Compared with the raw returns, the residuals exhibit a distribution that is closer to normality, indicating that the GARCH filtering successfully captures a substantial portion of the time-varying volatility.

Figure 13 reports the out-of-sample volatility and risk forecasts obtained from the GARCH(1,1) model estimated on weekly exchange rate returns.

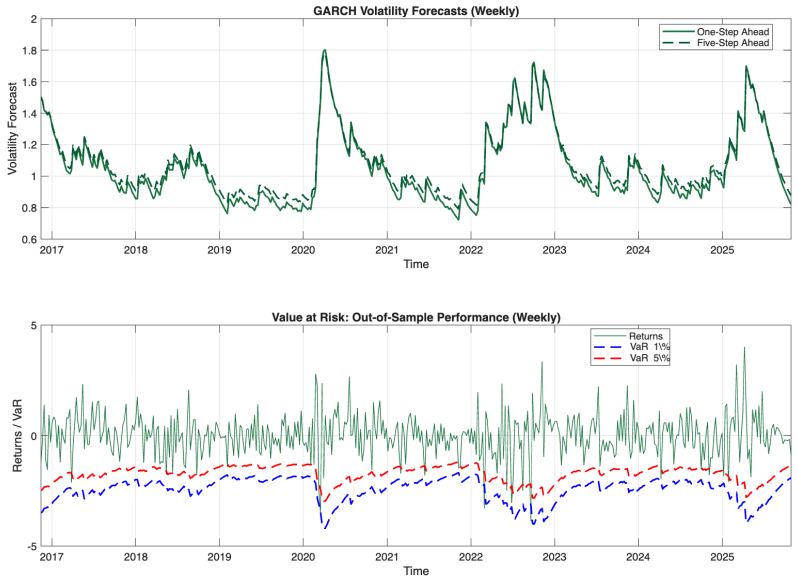

Figure 13: 1/5-Step Ahead Forecast and VaR at 1% and 5% levels

The upper panel shows the one-step-ahead and five-step-ahead conditional volatility forecasts. Both series display a high degree of persistence and closely track periods of heightened market uncertainty, such as the COVID-19 episode and subsequent phases of financial stress. As expected, the five-step-ahead forecast is smoother and less reactive to short-run fluctuations, reflecting the gradual convergence of multi-step forecasts towards the long-run variance implied by the model.

The forecasting accuracy of the conditional variance is summarized by the mean squared forecast error, which equals 3.278. While this value reflects the inherent difficulty of predicting volatility at the weekly horizon, the forecasts nonetheless capture the main swings in volatility and respond appropriately to large shocks.

The lower panel reports the one-step-ahead Value at Risk forecasts at the 1% and 5% confidence levels together with the realized returns. The VaR bands widen substantially during turbulent periods and contract during calmer phases, indicating that the risk forecasts adapt coherently to changes in the volatility environment.

Quantitative validation of the VaR forecasts confirms this visual evidence. At the 1% level, 3 exceedances are observed, corresponding to an empirical exceedance rate of 0.64%, which is below the nominal level of 1%. Similarly, at the 5% level, 21 exceedances are recorded, yielding an empirical exceedance rate of 4.49%, compared to the expected rate of 5%. In both cases, the number of exceedances is slightly lower than predicted, suggesting a mildly conservative behavior of the GARCH-based VaR forecasts.

4 Bootstrap Algorithm for ARCH(1) Likelihood ratio test

In this section, we outline the bootstrap methodology employed to conduct inference on the ARCH(1) model. Consider the data-generating process

$$\begin{cases} x_t = \sigma_t z_t, \\ \sigma_t^2 = \omega + \alpha x_{t-1}^2, \end{cases} \tag{3}$$

where $\{z_t\}$ is an i.i.d. sequence with zero mean and unit variance.

We are interested in testing the null hypothesis

$$H_0 : \alpha = \bar{\alpha} \quad \text{against} \quad H_1 : \alpha \neq \bar{\alpha}.$$

To assess this hypothesis, we adopt a *fitted bootstrap* approach. The bootstrap is designed to approximate the finite-sample distribution of the test statistic under the null hypothesis while preserving the dynamic structure of the original data-generating process. In particular, since the ARCH(1) model exhibits conditional heteroskedasticity and nonlinear dependence, resampling schemes that ignore the temporal recursion would fail to replicate its key features. For this reason, we rely on the **recursive bootstrap**, which explicitly mimics the ARCH dynamics and is therefore suitable for both estimation and hypothesis testing in conditional variance models. To assess the testing procedure, we rely on the likelihood ratio test, which is given by $LR = -2(\ell_n^{(1)} - \ell_n^{(0)})$.

Algorithm 1 Recursive Bootstrap Likelihood Ratio Test for the ARCH(1) Model

Require: Observed series $\{x_t\}_{t=1}^T$, null value $\bar{\alpha}$, number of bootstrap replications B

1: **Restricted estimation.** Estimate the ARCH(1) model under the null hypothesis $H_0 : \alpha = \bar{\alpha}$ and obtain the restricted estimator $\hat{\omega}_0$.

2: **Computation of standardized residuals.** Compute the conditional variance under the null,

$$\hat{\sigma}_{0,t}^2 = \hat{\omega}_0 + \bar{\alpha} x_{t-1}^2,$$

and form standardized residuals

$$\hat{z}_t = \frac{x_t}{\hat{\sigma}_{0,t}}.$$

Center and rescale $\{\hat{z}_t\}$ to have zero mean and unit variance.

3: **for** $b = 1, \ldots, B$ **do**

4: **Bootstrap data generation.** Generate a bootstrap sample $\{x_t^{*(b)}\}_{t=1}^T$ recursively according to

$$\sigma_t^{*(b)2} = \hat{\omega}_0 + \bar{\alpha}\big(x_{t-1}^{*(b)}\big)^2,$$
$$x_t^{*(b)} = \sigma_t^{*(b)} z_t^{*(b)},$$

where $\{z_t^{*(b)}\}$ are drawn with replacement from the centred standardized residuals, and the recursion is initialized at $x_0^{*(b)} = x_0$.

5: **Bootstrap test statistic.** Estimate the restricted and unrestricted ARCH(1) models on $\{x_t^{*(b)}\}$ and compute the likelihood ratio statistic

$$LR_n^{*(b)} = -2\big(\ell_n^{*(b,0)} - \ell_n^{*(b,1)}\big).$$

6: **end for**

7: **Bootstrap inference.** Approximate the sampling distribution of LR_n under H_0 by the empirical distribution of $\{LR_n^{*(b)}\}_{b=1}^B$ and compute

$$\hat{p}^* = \frac{1}{B}\sum_{b=1}^{B} \mathbb{I}\Big(LR_n^{*(b)} \geq LR_n\Big).$$

Theoretical Properties

Under the recursive bootstrap, the bootstrap observations are generated as

$$x_t^* = \sigma_t^* z_t^*,$$

where $\sigma_t^{*2} = \hat{\omega}_0 + \bar{\alpha}(x_{t-1}^*)^2$ and z_t^* is drawn with replacement from the centered standardized, where $z_t \sim i.i.d\,(0,1)$.

The bootstrap conditional mean satisfies

$$\begin{aligned}\mathbb{E}^*[x_t^* \mid \mathcal{I}_{t-1}] &= \mathbb{E}^*[\sigma_t^* z_t^* \mid \mathcal{I}_{t-1}] \\ &= \sigma_t^* \mathbb{E}^*[z_t^* \mid \mathcal{I}_{t-1}] \\ &= \sigma_t^* \frac{1}{T}\sum_{i=1}^{T}\left(\hat{z}_i - \bar{\hat{z}}\right) = 0,\end{aligned}$$

by construction of the centered bootstrap innovations. The bootstrap conditional variance is given by

$$\begin{aligned}\mathbb{V}^*[x_t^* \mid \mathcal{I}_{t-1}] &= \mathbb{E}^*[(x_t^*)^2 \mid \mathcal{I}_{t-1}] - (\mathbb{E}^*[x_t^* \mid \mathcal{I}_{t-1}])^2 \\ &= \mathbb{E}^*[(\sigma_t^* z_t^*)^2 \mid \mathcal{I}_{t-1}] \\ &= (\sigma_t^*)^2 \mathbb{E}^*[(z_t^*)^2 \mid \mathcal{I}_{t-1}] \\ &= (\sigma_t^*)^2 \frac{1}{T}\sum_{i=1}^{T}(\hat{z}_i - \bar{\hat{z}})^2 \\ &= (\sigma_t^*)^2\end{aligned}$$

About Bootstrap at the boundary

The use of bootstrap procedures in ARCH-type models must be treated with particular caution whenever inference is conducted at, or close to, the boundary of the parameter space. In the ARCH(1) model, estimation is typically carried out by constrained QMLE, since the admissible parameter space is given by

$$\Theta = \left\{\theta = (\omega, \alpha)' \in \mathbb{R}^2 : \omega > 0,\ \alpha \geq 0\right\}.$$

As a consequence, the null hypothesis $H_0 : \alpha = \bar{\alpha}$ may correspond to a boundary point of Θ, in particular when $\bar{\alpha} = 0$.

The validity of standard bootstrap procedures relies on the ability to transfer the convergence of the empirical distribution function to the convergence of the statistic of interest. In particular, after establishing uniform convergence of the empirical distribution function $\hat{F}_n$ to the true distribution F via the Glivenko–Cantelli theorem,

$$\sup_{x\in\mathbb{R}}\left|\hat{F}_n(x) - F(x)\right| \xrightarrow{\text{a.s.}} 0,$$

one typically invokes the *Continuous Mapping Theorem* (or, more generally, the functional delta method) to obtain convergence of the induced distribution of a statistic,

$$\hat{G}_n = \mathcal{T}(\hat{F}_n),$$

where $\mathcal{T}$ denotes the functional mapping the empirical distribution into the estimator or test statistic (e.g. the likelihood ratio statistic).

This step requires the mapping from the empirical distribution to the estimator and the test statistic to be continuous. However, when parameters lie on the boundary of the parameter space, this condition fails. In the ARCH(1) model the constraint $\alpha \geq 0$ implies that, when $\alpha_0 = 0$, the mapping to the QMLE and to the likelihood ratio statistic is no longer smooth.

At the boundary, the likelihood ratio statistic does not follow the standard χ_1^2 asymptotic distribution, in fact it converges to a nonstandard limit. As a result, the regularity conditions required for bootstrap validity are violated; therefore, when $\bar{\alpha} = \alpha_0 = 0$, both asymptotic and bootstrap-based likelihood ratio inference must be interpreted with caution.

Empirical Findings

In this section, we report the empirical results produced by the bootstrap procedure. The code generates (i) the bootstrap sampling distribution of the ARCH(1) parameter $\hat{\alpha}$ and (ii) a Gaussian finite-sample approximation, used as a benchmark to assess the adequacy of normal-based inference.

In our **MATLAB** implementation we simulate an ARCH(1) process of length $T = 1000$ under the parameter values $\omega = 0.012$ and $\alpha = 0.6$, with initial condition $x_1 = x_0 = 1$ and i.i.d. innovations $z_t \sim \mathcal{N}(0, 1)$. The simulated series is generated recursively according to

$$\sigma_t^2 = \omega + \alpha x_{t-1}^2, \qquad x_t = \sigma_t z_t, \qquad t = 2, \ldots, T,$$

with $\sigma_1^2 = \omega + \alpha x_1^2$. We then estimate an ARCH(1) model (implemented as `garch(0,1)`) by Gaussian QMLE using `estimate`, obtaining $\hat{\omega}$, $\hat{\alpha}$ and their (asymptotic) standard errors.

To study finite-sample behaviour, we next compute standardized residuals $\hat{z}_t = x_t/\hat{\sigma}_t$ and construct a *recursive residual bootstrap*. For each replication $b = 1, \ldots, B$ with $B = 999$, we resample z_t^* from the centered and standardized empirical residuals and generate a bootstrap series $\{x_t^{*(b)}\}$ through the same ARCH recursion using the fitted parameters. Re-estimating the model on each bootstrap sample yields draws $\{\hat{\alpha}^{*(b)}\}$, which we use to approximate the sampling distribution of $\hat{\alpha}$ and to compare its ECDF with a Gaussian benchmark.

Finally, we implement a bootstrap likelihood ratio (LR) test of

$$H_0 : \alpha = \bar{\alpha},$$

setting $\bar{\alpha} = 0.6$ in the code. We compute the observed LR statistic

$$LR_{\text{obs}} = -2\big(\ell^{(0)} - \ell^{(1)}\big),$$

where $\ell^{(0)}$ and $\ell^{(1)}$ denote the maximized log-likelihoods under the restricted and unrestricted models, respectively. We then generate bootstrap samples under H_0 (using the restricted estimate of ω) and recompute the bootstrap LR statistics $\{LR^{*(b)}\}_{b=1}^{B}$ to obtain the bootstrap p-value

$$\hat{p}^* = \frac{1}{B}\sum_{b=1}^{B} \mathbb{I}\Big(LR^{*(b)} \geq LR_{\text{obs}}\Big).$$

We also plot the empirical density of LR^* together with the asymptotic χ_1^2 density to highlight potential deviations from standard LR asymptotics in finite samples.

Figure 14a displays the bootstrap density of $\hat{\alpha}$ obtained from the replications $\{\alpha_b\}_{b=1}^{B}$. The distribution is clearly non-Gaussian: it is asymmetric and exhibits a relatively thick right tail, consistent with the well-known finite-sample behaviour of persistence parameters in conditional heteroskedasticity models. In particular, mass accumulating near the upper boundary (e.g. close to 1) is a typical symptom of boundary and near-nonstationarity effects, implying that standard normal approximations for $\hat{\alpha}$ may be unreliable.

Figure 14b compares the empirical CDF of the bootstrap draws with the Gaussian CDF calibrated at $(\mu, \sigma) = (\,\hat{\alpha},\, \widehat{\text{sd}}(\alpha_b)\,)$. The two curves differ substantially over most of the support: the bootstrap ECDF is shifted to the right and departs from the smooth Gaussian benchmark. This discrepancy confirms that the finite-sample distribution of $\hat{\alpha}$ is not well captured by a normal approximation, motivating bootstrap-based inference for testing and confidence intervals.

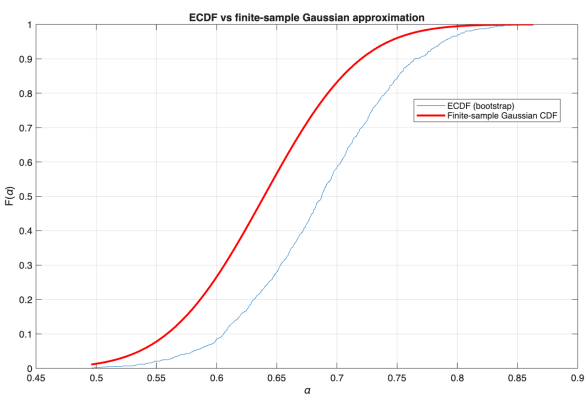

(a) Bootstrap density (histogram) of $\hat{\alpha}$.

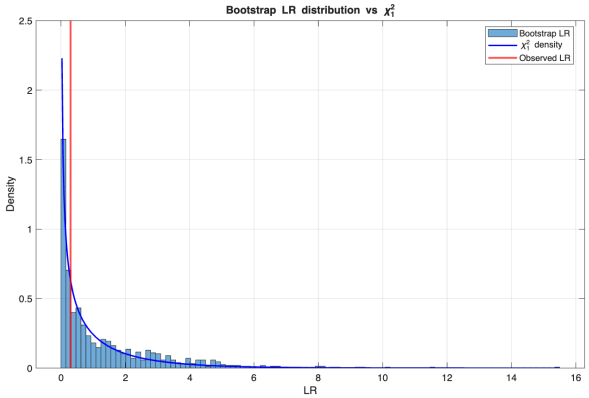

(b) ECDF of $\hat{\alpha}$ versus Gaussian CDF benchmark.

Figure 14: Finite-sample behaviour of the ARCH(1) coefficient estimator: bootstrap distribution and comparison with a Gaussian approximation.

References

[Bollerslev, 1986] Bollerslev, T. (1986). Generalized autoregressive conditional heteroskedasticity. *Journal of Econometrics*, 31(3):307–327.

[Glosten et al., 1993] Glosten, L. R., Jagannathan, R., and Runkle, D. E. (1993). On the relation between the expected value and the volatility of the nominal excess return on stocks. *Journal of Finance*, 48(5):1779–1801.

[Loretan and Phillips, 1994] Loretan, M. and Phillips, P. C. B. (1994). Testing the covariance stationarity of heavy-tailed time series. *Journal of Empirical Finance*, 1(2):211–248.